ORIGIN OF IRON-RICH BEDS IN THE BASAL WAJID SANDSTONE, ABHA–KHAMIS MUSHAYT AREA, SOUTHWEST SAUDI ARABIA

Lameed O. Babalola*
Center for Petroleum and Minerals, Research Institute

and

Mahbub Hussain and Mustafa M. Hariri
Earth Sciences Department

King Fahd University of Petroleum and Minerals
Dhahran 31261, Saudi Arabia

الخلاصــة

يظهر الجزء السفلي من مقطع حجر الرمل التابع لمتكون الوجيد في كل من منطقة أبها وخميس مشيط التابعتين لمحافظة عسير في جنوب غرب المملكة العربية السعودية . ويتمثل ذلك بعدد من المكاشف العلوية الصغيرة التي تعلو صخور الأساس التي تعود لحقبة البريكامبري والتي تتكون من الصخور النارية الجوفية والمتحولة المختلفة التي تشمل صخور الشيست ، والامفيبوليت ، والجرانيت ، والديورايت والجابرو . يصل سمك طبقة متكون الوجيد الرملي في منطقة الدراسة إلى ٣٠٠ م وهو يتكون غالباً من حجر الرمل المتوسط إلى خشن الحبيبات المُتقاطع التطبق . وقد قُسم الحجر الرملي هذا إلى وحدتين بناء على اللون والصفات الصخرية : (١) الوحدة الحمراء في الأسفل ، (٢) والوحدة الرمادية في الأعلى . وتمتاز الوحدة الحمراء بتوافر النطاقات الغنية بالحديد التي يُشار إليها بحجر الحديد في هذه الورقة ، بينما تفتقر الوحدة الرمادية إلى النطاقات الغنية بالحديد . ويتواجد حجر الحديد في الحقل على شكل حشوات للشقوق ، وأجزاء من طبقات الحجر الرملي بين الطبيقات التابعة لوحدة الحجر الرملي المتقاطع الطبيقات ، وكتكثفات وتجمعات عقدية من الحديد .

وقد أظهرت الاستقصاءات الجيوكيميائية للحجر الحديدي أن تركيز الحديد يتراوح بين ٩% أكثر من ١٥%. وكذلك أظهرت الدراسات البيتروغرافية (الميكرسكوبية) أن حجر الحديد عبارة عن حجر مرو الأرنيت (حجر رملي عالي التركيز من معدن المرو (الكوارتز)) ويتواجد الحديد فيه كمادة لاحمة تغطي حبيبات المرو (الكوارتز) المتوسطة إلى الخشنة التحبب. والمعدنان الرئيسيّان للحديد هنا هما الهيماتيت والجوثيت ويتكونان على شكل اما حشو للفرغات البينية أو مواد لاحمة تغلف الحبيبات. وقد يعود أصل الحديد في الحجر الحديدي هذا إلى العمليات المتأخرة في تكوين حجر الرمل ، وقد يبرهن على ذلك الإحلال الجزئي لمعدن الكالسيت اللاحم الأساسي بأكاسيد الحديد . كما أن الشكل السطحي البلوري الرقيق لمعادن الحديد من خلال ميكروسكوب الماسح الاليكتروني تؤيد هذا

*Address for Correspondence:
Research Institute
Center for Petroleum & Minerals
KFUPM Box 5040, King Fahd University of Petroleum and Minerals
Dhahran 31261, Saudi Arabia

الاستنتاج . والعلاقه السلبية بين عنصري الكالسيوم والحديد التي ظهرت بالدراسة الجيوكيميائية تُضيف أيضاً برهاناً آخر إلى أن الحديد قد حل محل الكالسيوم .

كما أبانت الدراسات الميكرسكوبية والجيوكيمائية أن نطاقات الحديد في حجر الحديد في حجر رمل الوجيد له مصادر متعددة منها تذوب قطع (١) المعادن الحديدومغنسيوم في ذات الحجر الرملي و (٢) تجوية صخور معقد الأساس (الدرع العربي) في المنطقة. كما قد يدلل تواجد العدد الكبير من عروق البجماتيت في صخور معقد الأساس ، قطع الجاسبار في الحجر الحديدي والظهور المشتت لنطاق معدن الكاؤليين في أعلى صخور الأساس قد يدلل كل ذلك على التجوية الشديدة و/ أو نشاط للمحاليل الساخنة في المنطقة . ويقترح أنه لربما أن اندفاع وهبوط المحاليل المائية الساخنة كان نشطاً خلال فور ترسب الوحدة الحمراء من الحجر الرملي . وبناءً على طريقة تكون النطاقات الغنية بالحديد في الحجر الرملي وشكل المعادن الحديد ومغنيسيوم في الحجر الرملي لربما تدلل أيضاً على أن المحاليل المائية الساخنة لم تساعد فقط في إذابة المعادن الحديد ومغنيسيوم في حجر رمل الوجيد ، بل لربما ساهمت في تدوير المحاليل الحاملة للحديد التي كونت حجر الحديد في حجر رمل الوجيد.

كلمات المفتاح: الوجيد ؛ حجر الحديد ؛ أصل ؛ الدراسة الميكرسكوبية ؛ جيوكيمياء

ABSTRACT

The basal section of the Wajid Sandstone, exposed in Abha and Khamis Mushayt area of Asir Province, southwest Saudi Arabia, is represented by several small outliers on a Precambrian basement complex comprising different metamorphic and igneous rocks including schist, amphobolite, granite, diorite, and gabbro. The Wajid Sandstone in the study area is up to 300 m thick and consists dominantly of coarse- to medium-grained cross-bedded sandstone. Based on color and lithologic characteristics, this Sandstone is divided into two informal units: (*i*) Red Unit (basal unit); and (*ii*) Grey Unit. The Red Unit is characterized by an abundance of iron-rich horizons (referred to as ironstone in this paper), while Grey Unit is significantly poorer in iron-rich horizons. The ironstone outcrops as fracture-fills, portions of sandstone beds, encrustrations on foresets of cross-bedded sandstone units, and as concretions and nodules.

Geochemical investigations show that the Fe concentrations of the ironstone range from 9% to over 15%. Petrography shows that the ironstone is an iron-cemented/coated medium- to coarse-grained quartz arenite. Hematite and goethite, which represent the dominant iron minerals, typically occur either as pore-fills or as grain-coating cements. A late diagenetic origin of the iron is indicated by the partial replacement of early calcite cement by iron oxides. Preservation of delicate morphologies of the iron minerals, as shown in scanning electron microscopy (SEM), also favors a late-diagenetic origin of the iron minerals in the ironstone. A negative correlation between Ca and Fe as determined by geochemical studies adds further to this conclusion. Petrographic and geochemical evidence also suggest that the iron in ironstone intervals in the Wajid Sandstone was derived from a number of sources including: (*i*) dissolution of the labile, ferromagnesian minerals in the Sandstone itself; and (*ii*) weathering of the basement complex in the area. The presence of numerous pegmatite veins in the underlying basement complex, clasts of jasper in the ironstone, and the sporadic occurrences of kaolin horizons atop of the basement complex indicate extensive weathering and/or hydrothermal activity in the area. It has been suggested that hydrothermal circulation was active during and immediately after the deposition of the Red Unit. Based on the mode of occurrence of the iron-rich horizons, and paucity of ferromagnesian minerals in the sandstone, it is likely that hot hydrothermal fluids not only helped dissolution of the labile ferromagnesian minerals in the Wajid Sandstone, but also drove the circulation of the iron-bearing fluids responsible for the formation of the ironstone.

Key Words: Wajid; Ironstone; Origin; Petrography; Geochemistry.

ORIGIN OF IRON-RICH BEDS IN THE BASAL WAJID SANDSTONE, ABHA–KHAMIS MUSHAYT AREA, SOUTHWEST SAUDI ARABIA

1. INTRODUCTION

The Wajid Sandstone (Ordovician–Permian) on the Arabian Shield is a medium- to coarse-grained siliciclastic unit forming as outliers on the peneplained surface of a dominantly Precambrian basement complex [1–3]. The abundance of iron (in the form of iron-rich horizons) in the Wajid Sandstone has been reported by a number of workers including Grenwood [4], Babalola [5], and Hussain *et al*. [6]. Hussain *et al*. [6] observed iron-rich horizons (ironstone as defined by James [7]) in the basal section of the Wajid Sandstone in the Abha–Khamis Mushayt area, Asir Province (longitudes 42° and 42° 53′E and latitudes 17° 50′ and 18° 15′N). Until now, there has been no detailed study of the origin of this ironstone. Based on detailed fieldwork, and petrographic and geochemical data, the present study explains the origin of this ironstone in Abha and Khamis Mushayt area (Figure 1).

2. METHOD OF STUDY

A total of twenty-nine (29) iron-rich samples were collected from different outcrops of the Wajid Sandstone in the study area. Samples were processed for thin-section petrographic and geochemical analyses. Thin section petrography, X-ray diffraction (XRD), and scanning electron microscopy (SEM) were used in identifying the mineralogy of the ironstones. Geochemical analysis, which involved inductive coupled plasma (ICP) and X-ray fluorescence (XRF), determined the major, minor, and trace element chemistry of the samples.

3. GEOLOGICAL SETTING OF THE STUDY AREA

The Abha and Khamis Mushayt area constitutes part of the Asir terrane, an oceanic terrane that occupies southwestern part of the Arabian Shield in Saudi Arabia [8, 9]. During the Precambrian to Early Cambrian the basement complex was subjected to compressional stress and subsequent peneplanation associated with the Idas Orogeny [10]. The Wajid Sandstone nonconformably overlies the deeply weathered, peneplaned surface of the Proterozoic basement complex [3, 11, 12]. Uplift and erosion, related to the Hercynian Orogeny, have also affected the early Paleozoic sequences in the area, as indicated by the presence of incised valleys [5].

Tertiary laterite, columnar basalt, sparse Quaternary basalt, and surficial materials overlie the Wajid Sandstone in the southeastern and west central parts of the Abha quadrangle. Intense weathering of the basalt is indicated by well-developed laterite horizons. Farther to the east, in Wadi Ad Dwasir area, the Wajid Sandstone is overlain by the Permian Khuff Formation.

3.1. Basement Complex

The basement complex in the area is part of the Asir terrane, an arc-derived terrane with rocks ranging in age from 850 to about 638 Ma [8]. In Abha–Khamis Mushayt area the basement complex made up of metamorphosed volcanic and sedimentary rocks of the Baish, Bahah, Jeddah, and Halaban Groups, as well as upper Proterozoic plutonic rocks ranging from gabbro to granite [1, 4, 8]. A recent study by Johnson *et al*. [13] suggests that volcanic/plutonic activity continued until 606 ± 2 Ma in the Asir terrane. Based on field evidence, especially the presence of pegmatite dykes in the basal part of the Wajid Sandstone and patchy kaolin horizons (of possible hydrothermal origin) in the interval between the basement and the Wajid Sandstone, Hussain *et al*. [14], argued for the continuation of plutonic/hydrothermal into the early Paleozoic.

3.2. Wajid Sandstone

The Abha–Khamis Mushayt area of Asir province is located near the southeastern margin of the Arabian Shield. Several outliers in the vicinity of the Al Souda National Park (42° 50′ 22″ E; 18° 09′ 47″ N), Al Habalah National Park (42° 44′ 42″ E; 17° 59′ 15″ N), and Ahd Rufaidah (42° 50′ 25″ E; 18° 09′ 32″ N) localities, represent the Wajid

Sandstone in this area. Kellog *et al*. [15] divided the Wajid Sandstone into four members: Dibsiyah, Sanamah, Khusayyayn, and Juwayl, separated by distinct unconformities. The effects of the Taconic, Acadian, and Hercynian orogenic events in the area is indicated by pronounced unconformity at the base of Sanamah, Khusayyan, and Juwayl Members [11].

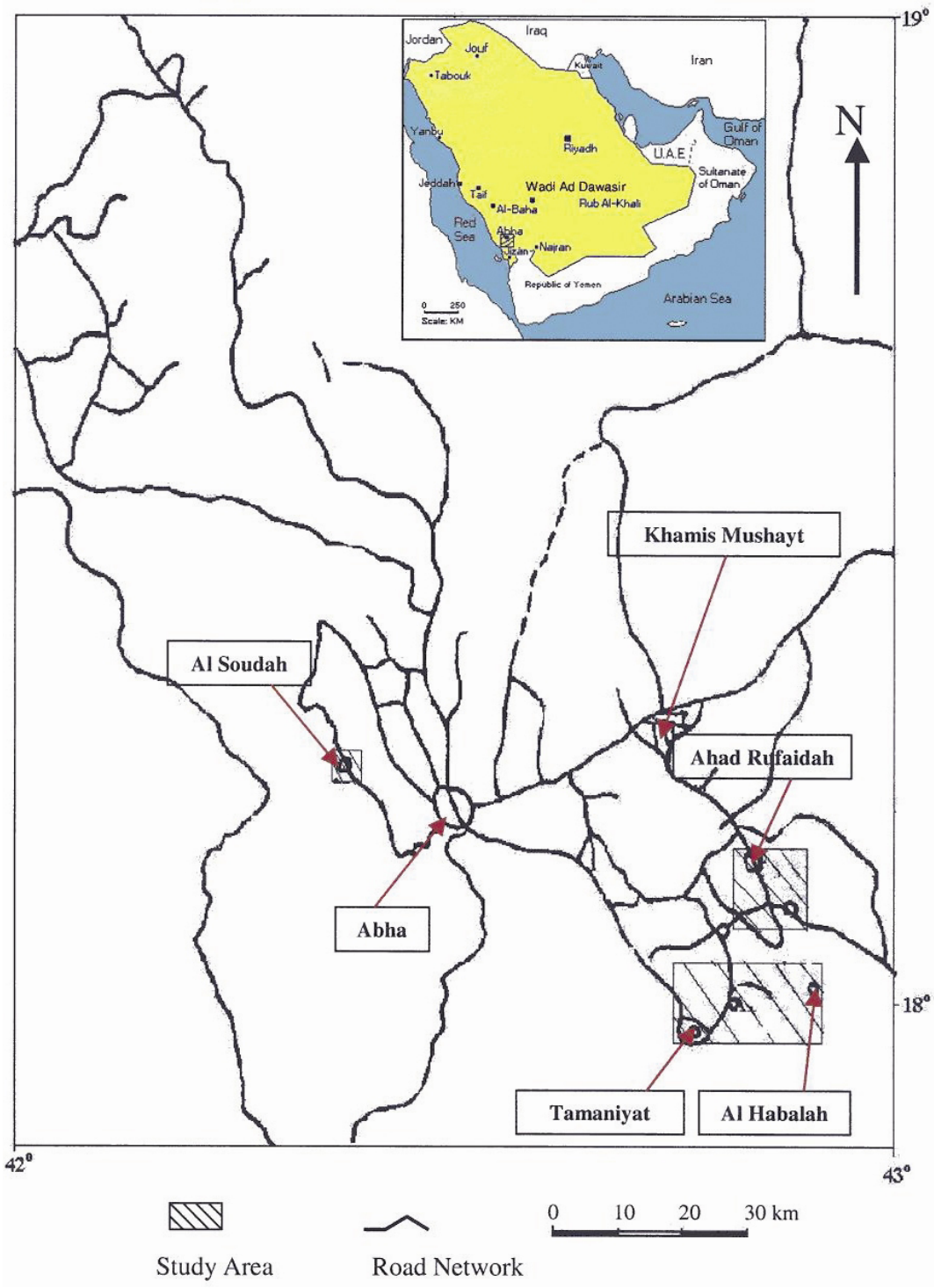

Figure 1. Location map of the study area. The outcrops studied represent several isolated hills or outliers of the Wajid Sandstone on the Arabian Shield in the vicinity of Abha and Khamis Mushayt, southwestern Saudi Arabia.

Stump and van der Eem [3] investigated the tectonic and sedimentation history of the Wajid Sandstone outcrop belt in the southwestern Saudi Arabia. According to them, the Wajid Sandstone in the area is represented by a variety of facies including shallow-marine, lagoon, braided river, fluviatile deltaic, and eolian. Greenwood [4], described a 235 m thick, tabular to wedge shaped, cross-bedded light brown to reddish–brown quartz-rich sandstone, characterized by iron-oxide concretions and layers.

The Wajid Sandstone in the study area is represented by an approximately 300 m thick sequence of dominantly coarse- to medium-grained massive to cross-bedded sandstone and kaolinite-rich silty claystone. Based mainly on the color and distribution of iron-rich horizons, the succession is informally divided into two units; a Red Unit (basal) and a Grey Unit, Figure 2 [5, 6]. The Red Unit composed of alternating successions of dominantly red–pink, occasionally brick red, grey to white, massive to cross-bedded sandstone with ironstone and kaolinite-rich claystone horizons. The Red Unit is separated from the overlying Grey Unit by an approximately 50 cm to 1 m thick conglomerate bed, comprising quartz and claystone clasts ranging in size from few mm to up to 10 cm. The Grey Unit is composed of a monotonous sequence of white–greyish, pebbly, coarse to medium, occasionally fine-grained, massive to cross-bedded sandstone. This unit is rich in white, friable kaolinite lenses and intraformational claystone clasts. Iron-rich beds observed are not common in the Grey Unit.

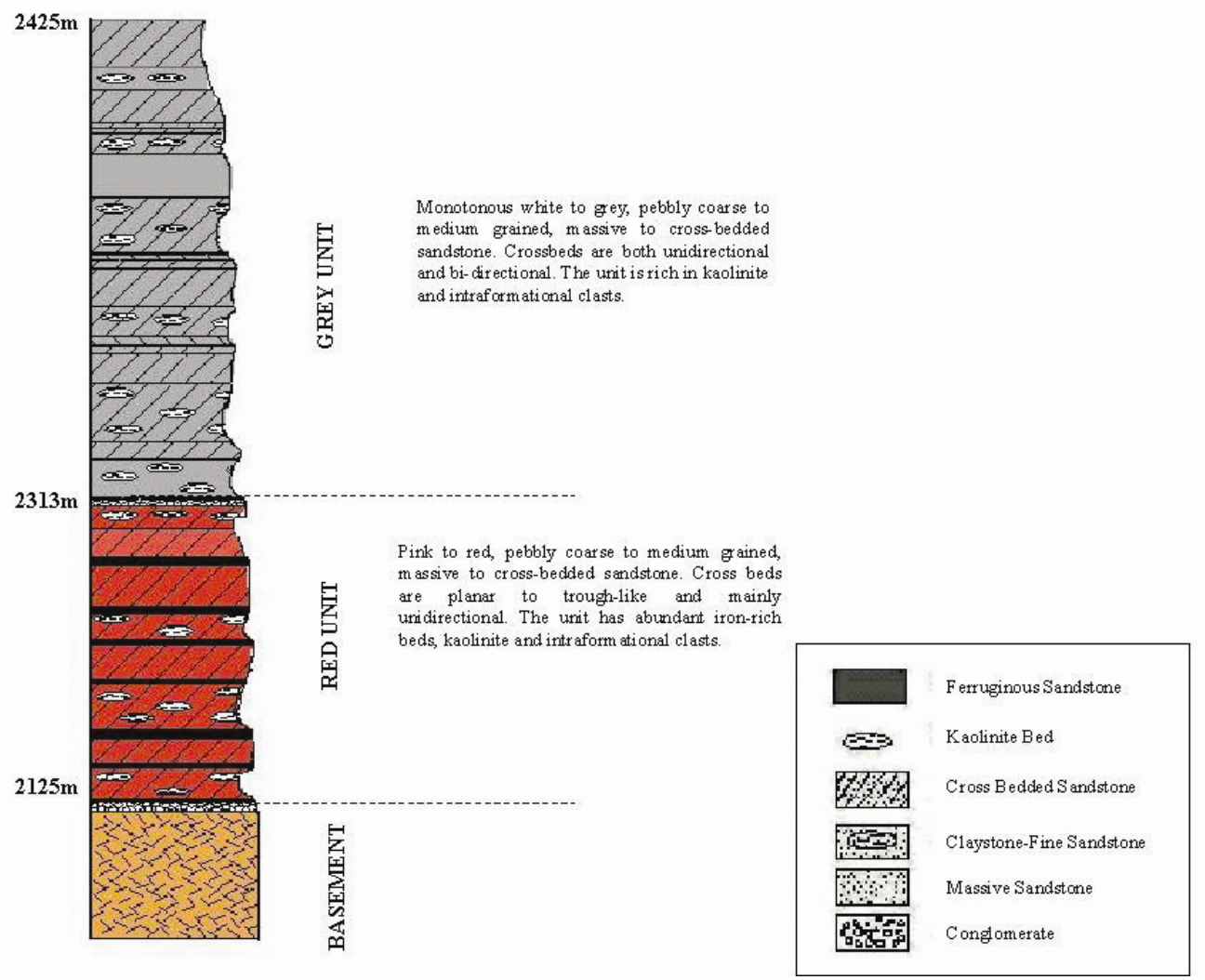

Figure 2. Stratigraphic column showing the lithology of the Wajid Sandstone. In the study area, the Wajid Sandstone non-conformably overlies the Precambrian basement complex.

4. IRONSTONE: FIELD OCCURRENCE

In outcrops, the iron-rich beds in the Wajid Sandstone show four distinct modes of occurrence: (*i*) thin beds ranging from a few centimeters to ~2 m thick, (*ii*) parts of the foresets of cross-bedded units, (*iii*) fracture infills, and (*iv*) concretions and nodules (Figure 3*a*–3*d*) reflecting differential cementation and matrix strength. Clasts of ironstones ranging in size from few mm to up to 10 cm are also common in recent (?) caliche that forms small patches atop mountain outcrops. Differential weathering of the ironstone and kaolinite-rich claystone occasionally forms caves with the more resistant, protruding ironstone intervals forming the roof of the caves. Well-rounded clasts (up to 8 cm in diameter) of vein quartz and jasper are common in ironstone horizons at Al Souda National Park area.

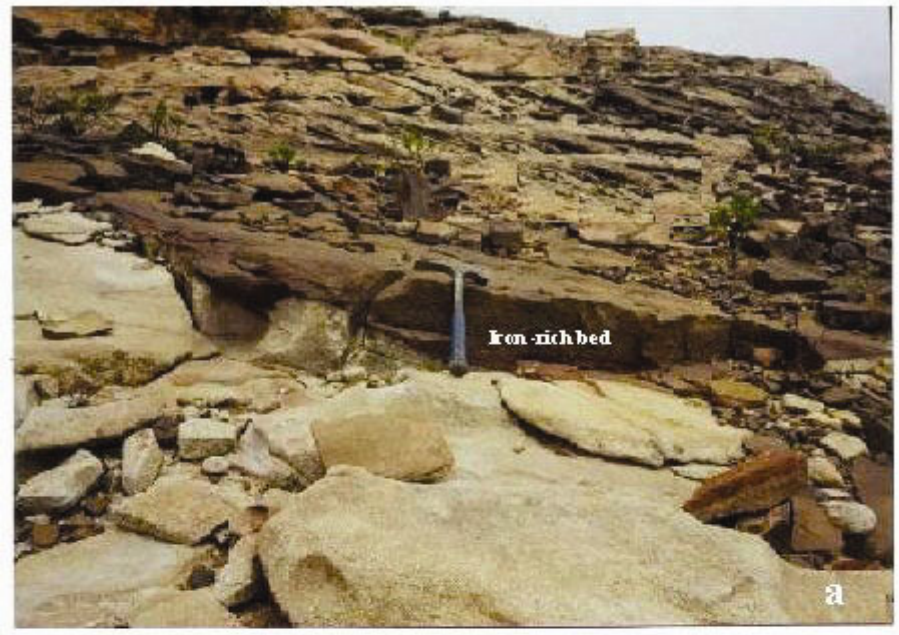

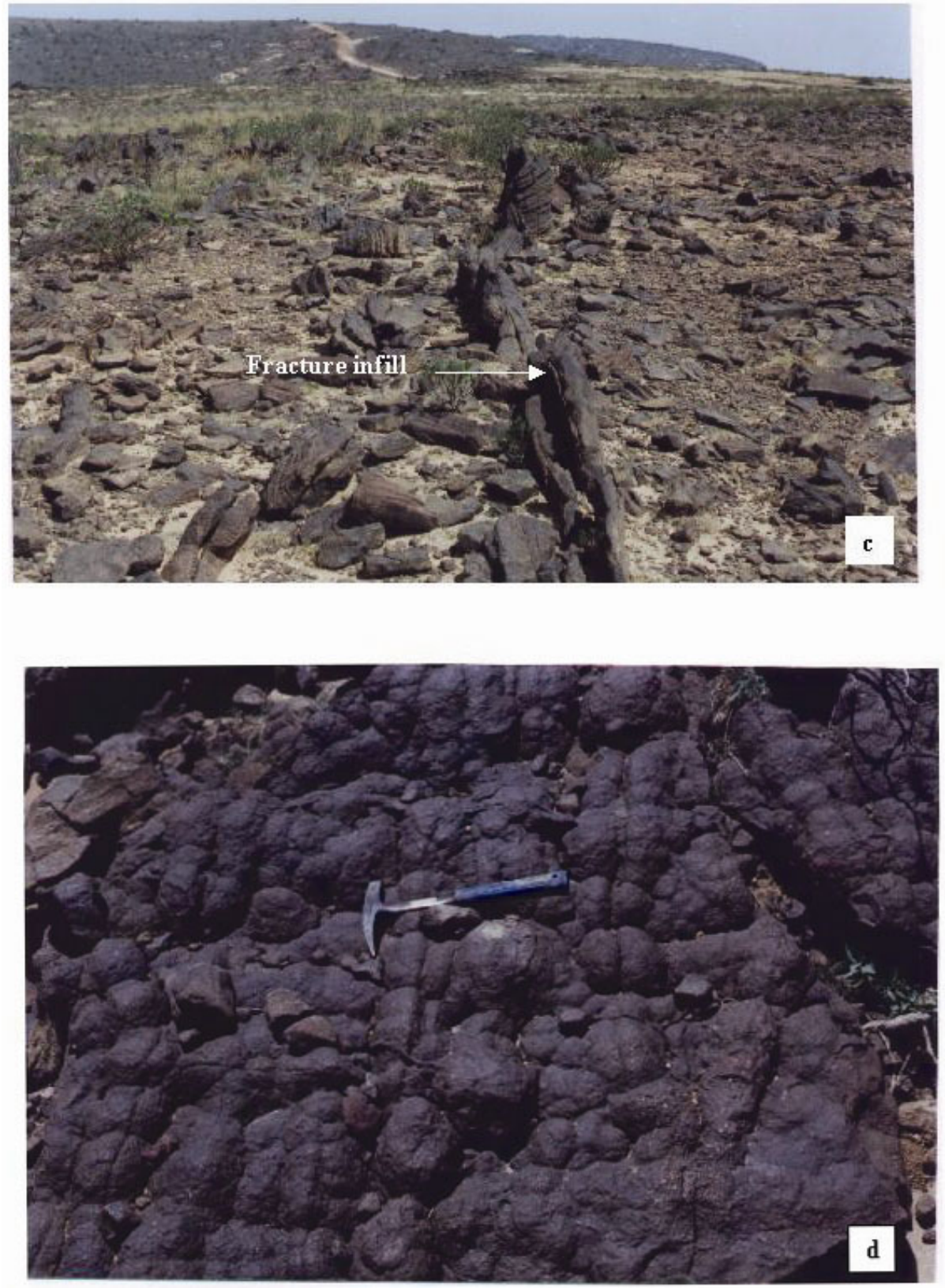

Figure 3. Modes of occurrence of iron rich horizons in the outcrops of the Wajid Sandstone: (a) *thin iron-rich bed;* (b) *part of a cross-bedded unit;* (c) *fracture infills; and* (d) *concretions and nodules.*

5. PETROGRAPHY

Thin-section petrography shows that, in general, the Wajid Sandstone is composed of angular to subrounded, poor to moderately well sorted, coarse- to medium-grained pebbly quartz-rich (>95% quartz) sandstone (Figure 4). Minor constituents include feldspars and rock fragments (mainly chert). A few highly degraded grains of feldspar and hornblende were also observed (Figure 5*a–d*). Silt-sized quartz grains and clay dominate the matrix.

Calcite is the dominant, and most likely the primary, cement in the Wajid Sandstone (Figure 6*a*). Iron oxides are the dominant cements in the ironstone samples. Samples with abundant iron are characterized by floating-grain textures (Figure 6*c*). Calcite is either absent or poorly developed in the iron-rich samples. This inverse relationship between calcite and iron-cements, coupled with the presence of traces of calcite in iron-cemented sandstones (ironstones), suggests replacement of earlier calcite cement by iron-rich cement. SEM investigations show that the iron minerals in the samples occur either as pore-filling cements or as grain coats (Figure 7*a*). Some delicate spherular iron minerals, mostly hematite in composition, were also observed (Figure 7*b*). Preservation of such delicate morphological and textural features would not be likely if the iron minerals were transported from a distant source. Based on the mode of occurrence (pore-filling and grain-lining cement) and preservation of delicate textural and morphological features, the iron minerals forming the ironstone are thought to be diagenetic, and formed in part by an in-situ replacement of an earlier calcite cement. The XRD data defined hematite, goethite, and chamosite as the main iron minerals in the ironstone cement (Table 1).

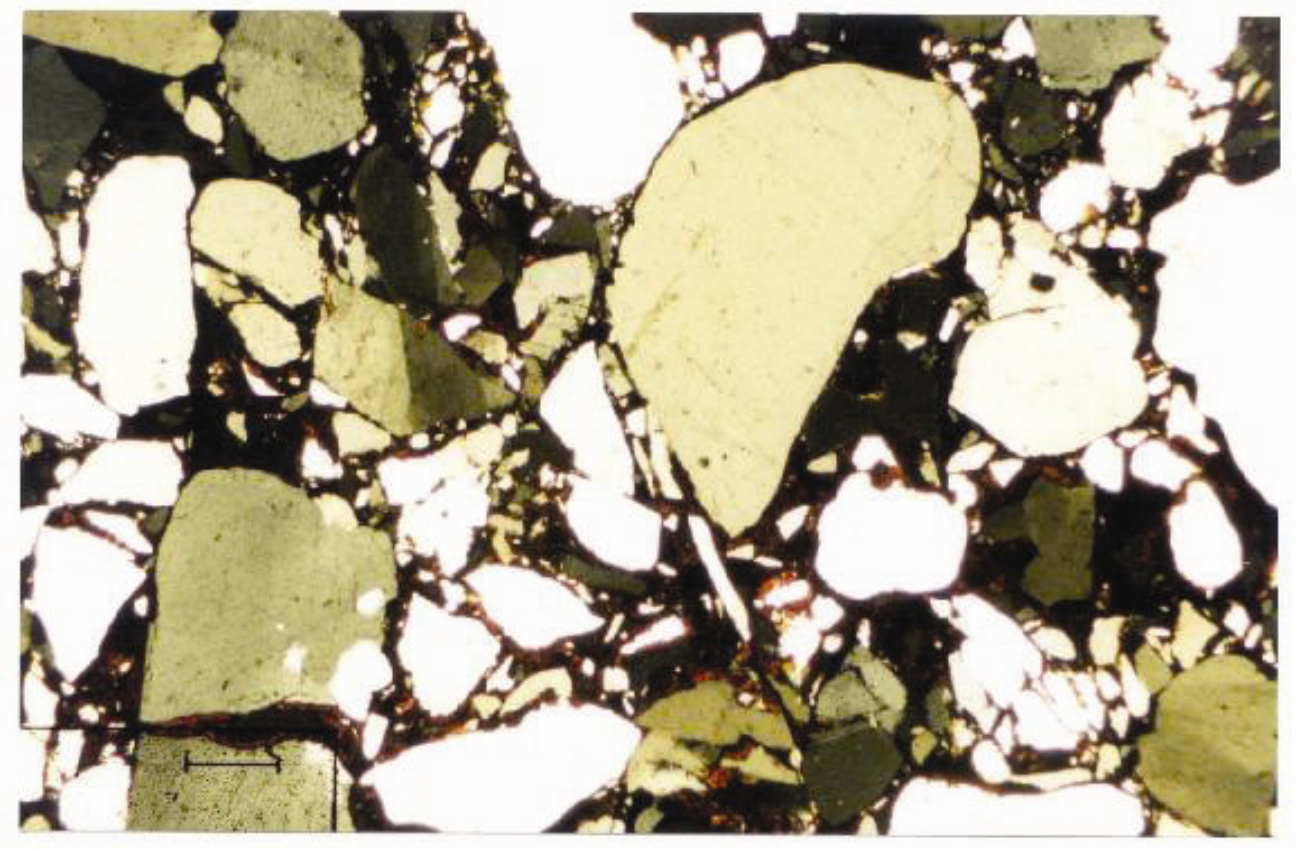

Figure 4. Photomicrograph showing typical mineralogical composition of iron-rich sample in the Wajid Sandstone (×125). The Wajid Sandstone is composed of angular to subrounded, pebbly coarse- to medium-grained, poor to moderately well sorted, quartz-rich sandstones.

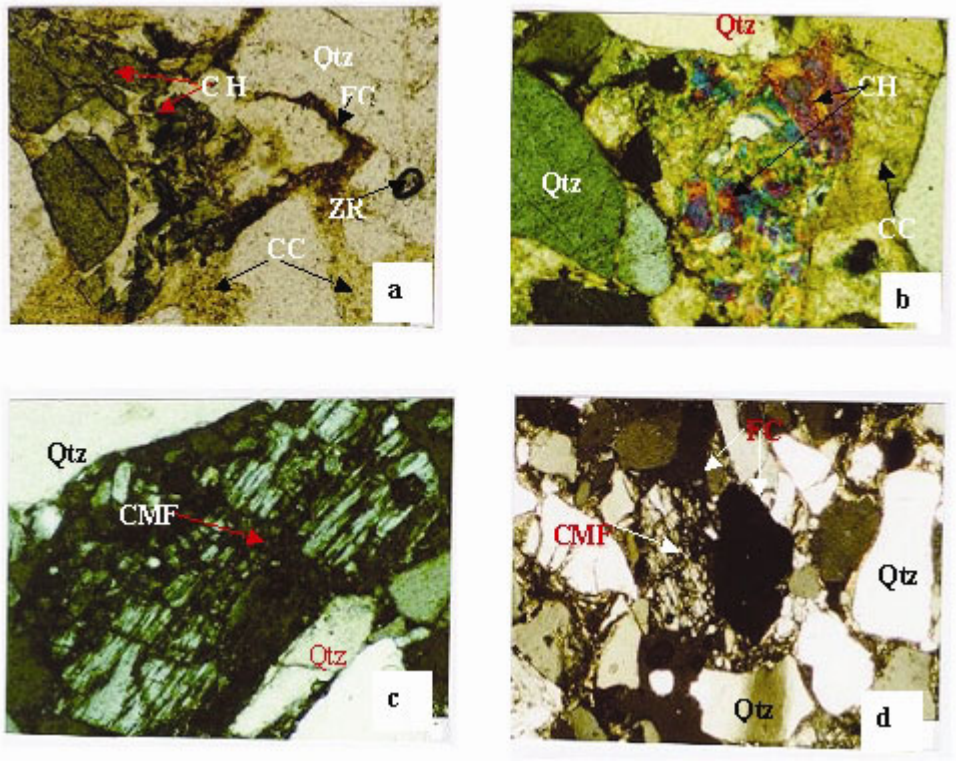

Figures 5. Photomicrographs showing degraded (corroded) minerals in the Wajid Sandstone: (a) *and* (b) *corroded hornblende (CH) grains embedded in calcite (CC) cement (×40). Note the presence of a zircon (ZR) grain as inclusion in a quartz grain in Figure* (a), (c), *and* (d). *Corroded microcline feldspar (CMF) grains (×40 and ×125 in* (c) *and* (d) *respectively). The degraded nature of these grains (hornblende and feldspar) suggests part of the iron in the Wajid Sandstone derived from dissolution of labile minerals in the sandstone. FC and Qtz represent ferruginous cement and quartz grains respectively.*

Table 1. Relative Distribution of Minerals in the Iron-Rich Samples in the Wajid Sandstone, Determined by X-ray Diffraction Analysis.

Note the dominance of quartz and significant presence of hematite, goethite, and kaolinite in the analyzed samples.

Sample	Quartz (%)	Goethite (%)	Hematite (%)	Kaolinite (%)	Calcite (%)	Chamosite (%)
AR15	97	3				
AR19	93		2			2
AR21	89		2	2	5	
AR22	96		1	2	1	
HA24	95	2	1	2		
HA27	96	2				2
OUT5I2	94	3	3			
OUT6I	80	9	1	10		
S2	96		2	2		
S20	95	5				
S28	98		2			
S39	95	5				

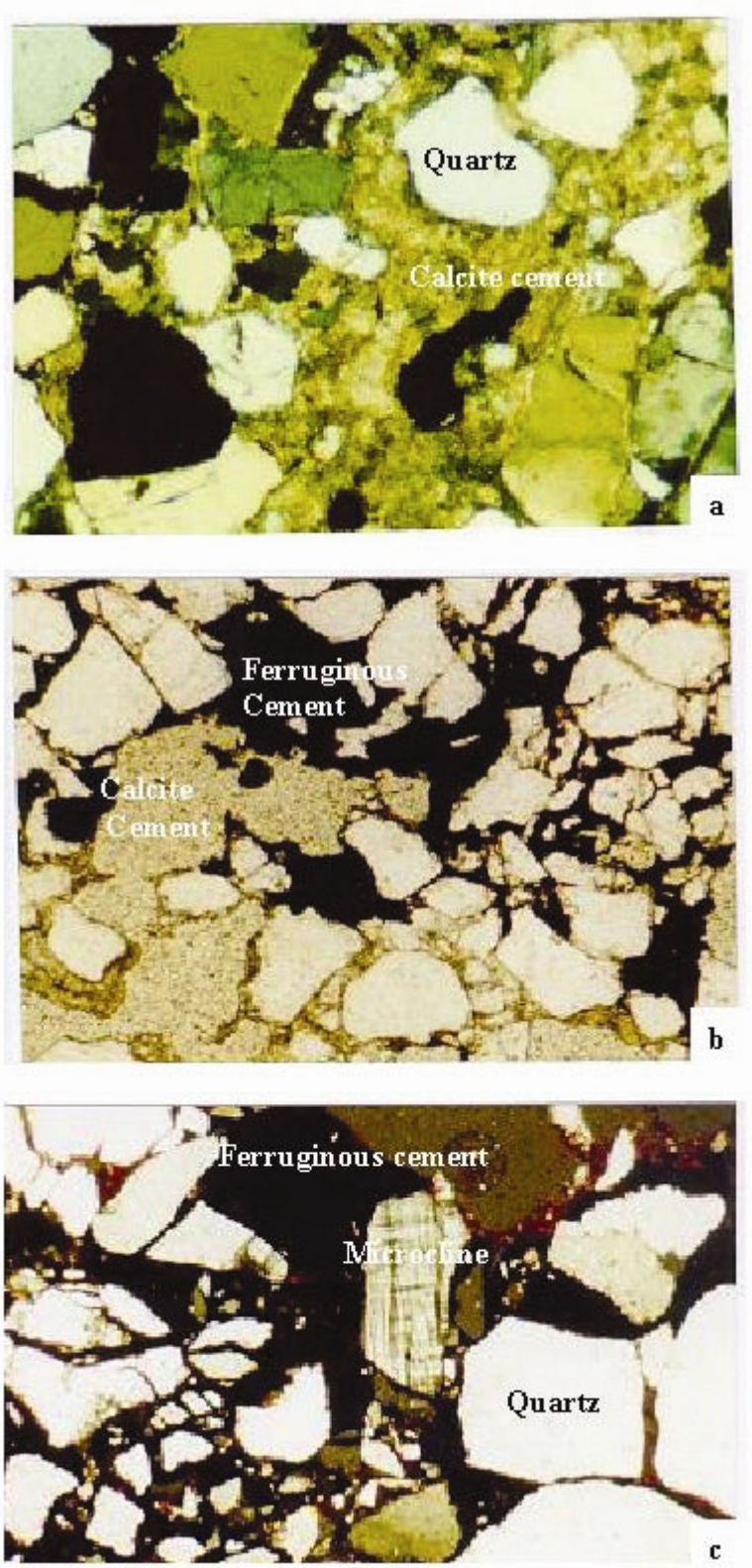

Figure 6. Photomicrographs showing different types of cements in the Wajid Sandstone: (a) *typical primary calcareous cement (calcite) in the Wajid Sandstone;* (b) *coexisting calcite and hematite cements. Note the replacement of early calcite cement by hematite in the Red Unit;* (c) *abundant iron cement (mainly hematite and goethite) impacts a floating grain texture in part of the Wajid Sandstone (×40).*

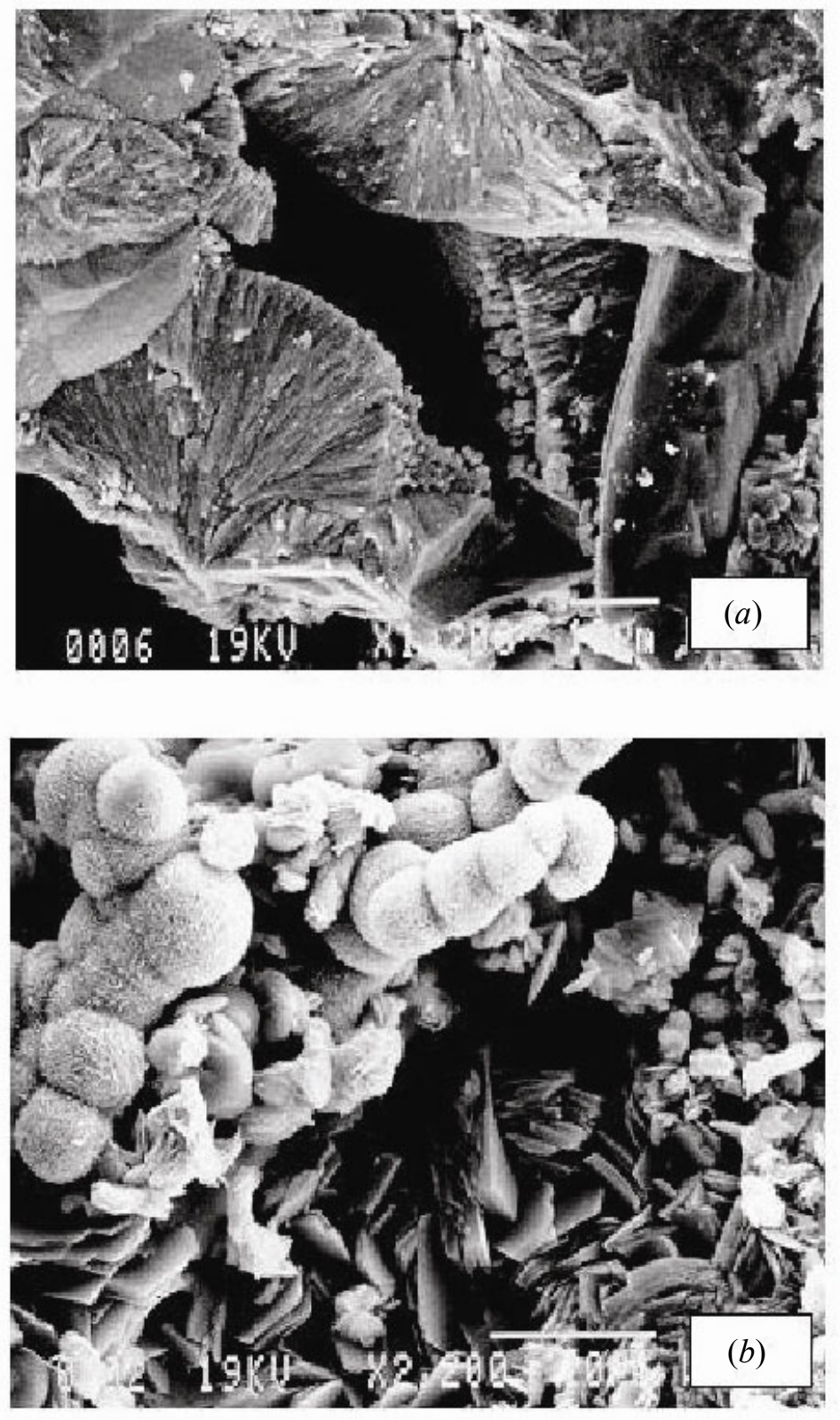

Figure 7. Scanning electron (SEM) photomicrographs showing morphological details of the ferruginous cement in the Wajid Sandstone: (a) *fan-shaped; and* (b) *spherular hematite in the Wajid Sandstone. The delicate nature of these textural morphologies suggests authigenic origin of these iron minerals.*

Table 2. Elemental Chemistry of the Iron-Rich Samples in the Wajid Sandstone.

The values of the chemical index of alteration (CIA) are also included in the last column of the table.

Sample	Al (%)	Ag (ppm)	As (ppm)	Ba (ppm)	Be (ppm)	Ca (%)	Co (ppm)	Cr (ppm)	Cu (ppm)	Fe (%)	K (%)	Mg (%)	Mn (ppm)	Mo (ppm)	Na (%)	Ni (ppm)	P (ppm)	Pb (ppm)	Sc (ppm)
AR3	0.41	<0.2	14	20	0.5	0.13	9	81	3	12.8	<0.01	0.06	1455	4	<0.01	12	270	8	1
AR9A	0.23	0.2	24	740	0.5	0.35	17	63	3	8.9	0.06	0.04	>10000	6	<0.01	12	1520	14	<1
AR15	0.26	0.2	<2	10	0.5	0.14	4	46	<1	11.7	<0.01	0.01	220	1	<0.01	13	50	6	1
AR19	0.18	0.2	2	30	1	0.34	3	95	3	>15	<0.01	0.06	70	2	0.01	5	310	6	2
AR25	0.14	<0.2	2	<10	<0.5	1.92	<1	24	1	3.21	<0.01	0.2	55	<1	<0.01	3	20	2	<1
ARLC3SC	0.27	<0.2	6	<10	<0.5	1.81	<1	75	<1	12.65	<0.01	0.03	10	2	<0.01	4	220	<2	1
HA14	<0.2	0.23	6	10	<0.5	0.11	4	57	7	1.17	<0.01	<0.01	90	3	<0.01	13	80	<2	1
HA18	0.13	<0.2	4	<10	<0.5	1.47	<1	29	5	2.75	<0.01	0.04	50	1	<0.01	5	10	<2	<1
HA24	0.21	0.2	8	30	0.5	0.06	7	68	9	12.2	<0.01	<0.01	285	<1	<0.01	19	140	<2	5
HA27	0.28	<0.2	2	10	<0.5	0.09	1	133	4	14.2	<0.01	0.01	20	1	<0.01	5	40	<2	1
HA36	0.35	<0.2	<2	<10	<0.5	0.14	1	48	4	3.82	0.01	0.05	35	3	0.01	10	40	2	1
HA51	0.2	0.2	<2	<10	<0.5	2.09	4	66	8	3.59	<0.01	0.04	50	1	<0.01	11	80	<2	1
HA56	<0.2	0.22	2	<10	<0.5	0.07	<1	56	1	1.45	<0.01	<0.01	15	<1	<0.01	2	40	<2	<1
HAP28	0.22	<0.2	<2	10	0.5	0.11	3	67	3	2.27	0.01	<0.03	80	<1	<0.01	7	60	2	<1
HAP31	0.27	0.2	<2	30	0.5	0.3	3	105	3	2	<0.01	0.01	105	1	0.02	6	100	10	2
OUT5I1	0.09	0.2	10	<10	1.5	0.09	14	81	12	7.82	<0.01	0.01	130	<1	<0.01	57	100	2	4
OUT5I2	0.11	<0.2	16	<10	2.5	0.42	3	79	6	9.6	<0.01	0.03	50	<1	<0.01	7	250	2	3
OUT6I	0.48	<0.2	2	<10	<0.5	0.16	<1	64	3	11.05	<0.01	0.05	15	1	<0.01	4	50	<2	1
S1	0.16	<0.2	6	<10	0.5	0.03	4	42	11	9.91	<0.01	<0.01	110	<1	<0.01	15	230	2	1
S5	0.12	<0.2	<2	<10	<0.5	0.06	<1	76	4	6.59	<0.01	0.01	20	1	<0.01	3	30	<2	<1
S12	0.15	3	16	30	0.5	0.03	5	42	10	3.19	<0.01	<0.01	210	6	<0.01	15	200	8	1
S13	0.19	4.2	<2	<10	<0.5	0.05	2	31	6	2.37	<0.01	0.01	25	1	<0.01	10	150	2	2
S13B	0.09	<0.2	<2	10	0.5	0.64	2	52	6	6.52	<0.01	0.01	105	3	<0.01	7	120	2	<1
S15	0.31	<0.2	<2	10	0.5	0.1	4	64	2	7.84	<0.01	0.01	180	<1	<0.01	8	220	<2	3
S20	0.12	<0.2	<2	10	2.5	0.03	4	75	6	10.6	<0.01	<0.01	95	<1	<0.01	13	120	<2	<1
S26	0.2	<0.2	8	30	0.5	0.16	4	52	3	9.7	<0.01	<0.01	185	11	<0.01	8	510	18	1
S28	0.16	<0.2	<2	<10	0.5	0.04	2	49	1	12.45	<0.01	<0.01	25	<1	<0.01	3	110	6	3
S30	0.18	0.2	<2	<10	0.5	<0.01	3	39	3	10.6	<0.01	<0.01	55	<1	<0.01	5	80	<2	<1
S39	0.08	0.2	<2	<10	0.5	0.01	4	24	1	12.8	<0.01	<0.01	140	<1	<0.01	9	40	<2	<1
Average	**0.207**	**0.727**	**8**	**70**	**0.806**	**0.391**	**4.65**	**6.48**	**4.74**	**7.89**	**0.03**	**0.04**	**138.75**	**2.82**	**0.13**	**10.03**	**179**	**5.75**	**1.84**

Sample	Sr (ppm)	Ti (%)	V (ppm)	Zn (ppm)	Al_2O_3 (%)	CaO (%)	Cr_2O (%)	Fe_2O_3 (%)	K_2O (%)	MgO (%)	MnO (%)	Na_2O (%)	P_2O_5 (%)	SiO_2 (%)	TiO_2 (%)	LOI (%)	TOTAL	CIA
AR3	15	<0.01	12	8	3.14	0.32	0.01	18.56	0.04	0.12	0.2	0.03	0.05	72.5	0.08	3	98.93	89
AR9A	87	<0.01	10	8	3.16	0.47	0.01	12.79	0.22	0.07	1.58	0.04	0.24	75.5	0.21	3.83	98.09	81.2
AR15	7	<0.01	6	10	2.09	0.25	<0.01	19.5	0.11	0.04	0.05	<0.01	0.03	73.9	0.11	3.54	99.58	85
AR19	20	0.03	103	4	2.53	0.6	<0.01	29	0.06	0.12	0.02	<0.01	0.09	64.4	0.12	2.26	99.18	79.1
AR25	59	0.02	8	<2	3.56	2.67	0.01	4.7	0.04	0.34	0.03	0.04	0.01	84	0.42	4.19	100	89
ARLC3SC	44	0.05	14	<2	16.74	2.83	0.03	19.82	0.09	0.11	0.01	0.03	0.01	50	0.98	8.81	99.45	85
HA14	5	<0.01	13	2	13.75	7.39	0.02	14.05	0.55	6.32	0.24	3.51	0.19	47.1	2.03	3.24	98.34	54.6
HA18	20	0.01	6	2	5.35	2.01	<0.01	3.94	0.04	0.04	0.01	<0.01	0.04	82.2	1.31	4.14	99.06	72.2
HA24	4	0.03	88	6	4.81	0.11	<0.01	21.49	0.05	<0.01	0.07	<0.01	0.04	68.5	0.34	3.64	99.04	96.6
HA27	17	0.02	10	6	2.46	0.16	<0.01	25.55	0.03	0.01	0.05	<0.01	0.04	66.9	0.17	3.73	99.14	92.5
HA36	14	0.01	15	2	22.54	0.2	<0.01	5.85	0.07	0.1	0.01	<0.01	0.12	59.8	0.44	9.64	98.77	98.8
HA51	6	0.01	22	4	3.68	2.85	<0.01	5.24	0.04	<0.01	0.01	<0.01	<0.01	79.6	0.23	7.41	99.07	55.9
HA56	5	<0.01	16	<2	9.48	0.11	<0.01	2.04	0.06	0.01	<0.01	<0.01	0.02	82.7	0.66	3.75	98.78	98.1
HAP28	7	0.01	41	2	3.03	0.14	0.01	3.17	0.08	0.08	0.02	0.05	0.01	90	0.25	2	98.79	91.8
HAP31	14	<0.01	77	6	0.85	42.4	<0.01	2.19	0.03	0.18	<0.01	<0.01	0.05	20.1	0.03	33.78	99.6	97.7
OUT5I1	6	<0.01	108	18	0.94	0.15	<0.01	16.46	0.03	<0.01	0.02	<0.01	<0.01	79.8	0.04	1.54	98.96	83.2
OUT5I2	3	0.01	37	10	1.14	0.67	<0.01	16.4	0.04	0.04	0.03	<0.01	0.03	79	0.1	1.69	99.15	61.3
OUT6I	8	0.05	9	<2	11.57	0.24	<0.01	16.55	0.05	0.07	0.03	<0.01	0.05	63.7	0.48	6.82	99.57	97.5
S1	5	<0.01	28	10	0.95	0.06	<0.01	24.99	0.03	<0.01	0.01	<0.01	0.1	70	0.06	2.98	99.17	91.3
S5	3	<0.01	1	<2	0.57	0.11	<0.01	15.81	0.03	<0.01	0.03	<0.01	0.1	80.1	0.09	2.27	99.15	78.2
S12	3	0.01	16	8	3.1	0.02	0.01	4.1	0.06	0.02	0.07	0.04	0.04	89.5	0.06	2.06	99.15	96.3
S13	4	0.01	16	4	15.72	0.05	0.01	3.3	0.07	0.05	0.01	0.03	0.04	71.5	0.68	6.67	98.11	99.1
S13B	7	<0.01	10	8	1.08	0.96	<0.01	17.09	0.03	<0.01	0.03	<0.01	0.08	76.7	0.21	3.07	99.2	51.9
S15	6	<0.01	3	10	2.14	0.17	<0.01	12.54	0.06	0.01	0.03	<0.01	0.07	81.4	0.07	2.78	99.3	89.9
S20	3	<0.01	13	12	0.69	0.06	<0.01	22.02	0.03	<0.01	0.02	<0.01	0.03	73.3	0.09	2.9	99.12	87.3
S26	7	<0.01	28	8	2.31	0.25	<0.01	17.44	0.04	<0.01	0.04	<0.01	0.17	77	0.09	2.27	99.64	88.5
S28	4	<0.01	82	<2	1.58	0.08	<0.01	23.18	0.04	<0.01	0.01	<0.01	0.05	72.5	0.06	1.74	99.26	93.4
S30	1	<0.01	10	10	1.33	0.03	<0.01	21.57	0.03	<0.01	0.01	<0.01	0.04	73.2	0.09	2.91	99.23	95
S39	<1	<0.01	9	10	0.39	0.04	<0.01	25.87	0.02	<0.01	0.03	<0.01	0.03	69.4	0.05	3.34	99.12	84.8
Average	**13.71**	**0.021**	**27.97**	**7.3**	**4.85**	**2.26**	**0.01**	**14.7**	**0.07**	**0.43**	**0.1**	**0.47**	**0.07**	**71.5**	**0.33**	**4.83**	**991.1**	**85**

CIA: Chemical Index of Alteration expressed by $[Al_2O_3/(Al_2O_3 + CaO + Na_2O + K_2O)]*100$

LOI: Loss on Ignition

AR: Ahad Rufaidah area; HA: Al -Habalah area I; HAP: Al-Habalah area II; S: Al-Soudah area;

OUT5I and OUT6I: Unlabeled iron-rich samples from outcrops 5 and 6 respectively in the Al-Habalah area.

(*a*)

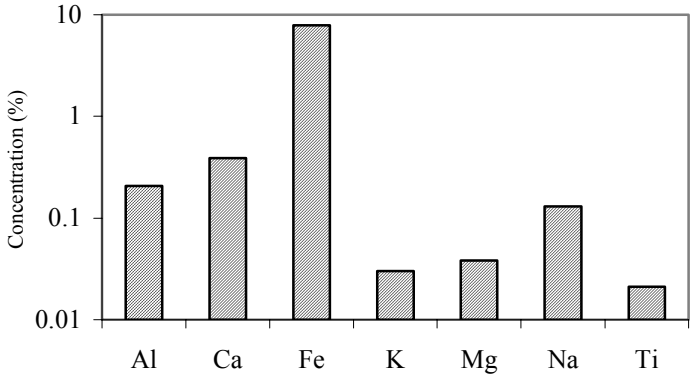

(*b*)

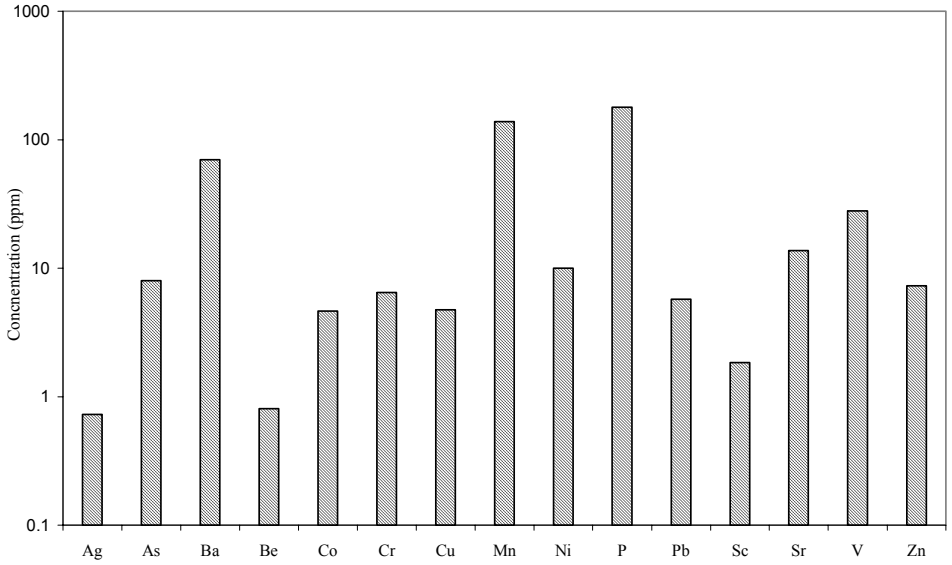

(*c*)

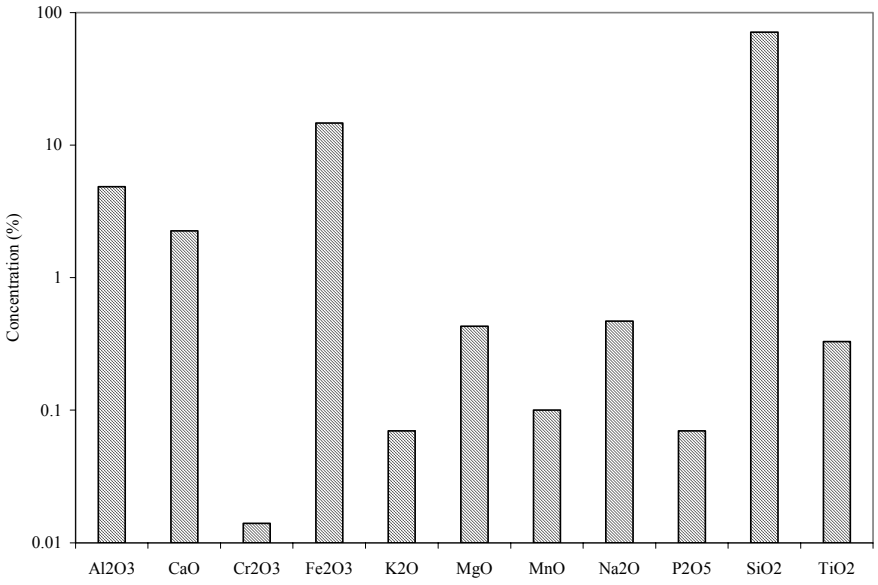

Figure 8. Relative distribution of different elements in the iron-rich samples in the Wajid Sandstone: (a) *major elements;* (b) *trace elements; and* (c) *selected elements as oxides. Note exceptionally high concentrations of Fe and* Fe_2O_3.

6. GEOCHEMISTRY

Except for Fe, the concentrations of major elements in the analyzed iron-rich samples are low (Table 2 and Figure 8). The concentrations of iron in the samples mostly range between ~9 and >15% (Fe_2O_3 is up to 29%). The concentrations of Al and Ca are low, ranging between 0.08 and 2.09% while Mg, K, Ti, and Na vary from <0.01 to 0.06. Except for a few samples, the concentration of Al_2O_3 and CaO are low, ranging from 0.34 to 6.32% and 0.04 to 2.83%, respectively. K_2O, TiO_2, and MnO values range from 0.01 and 2.03%. The concentrations of MgO, Na_2O, and P_2O_5 range from <0.01 to 0.09%. A variety of trace elements including Cr, Co, Ni, Cu, and V, common in mafic rocks are present (Figure 8).

The analytical data for Fe concentrations in the samples are consistent with the abundance of ironstone horizons in the Red Unit in the field. The low concentration of Ca in most of the samples (Table 2 and Figures 8 and 9) is also consistent with the replacement of calcite by hematite and goethite, as observed in thin section. The apparent high concentrations of Mn, as indicated by geochemical data (Table 2), may be due to the secondary co-enrichment of this element with Fe [16].

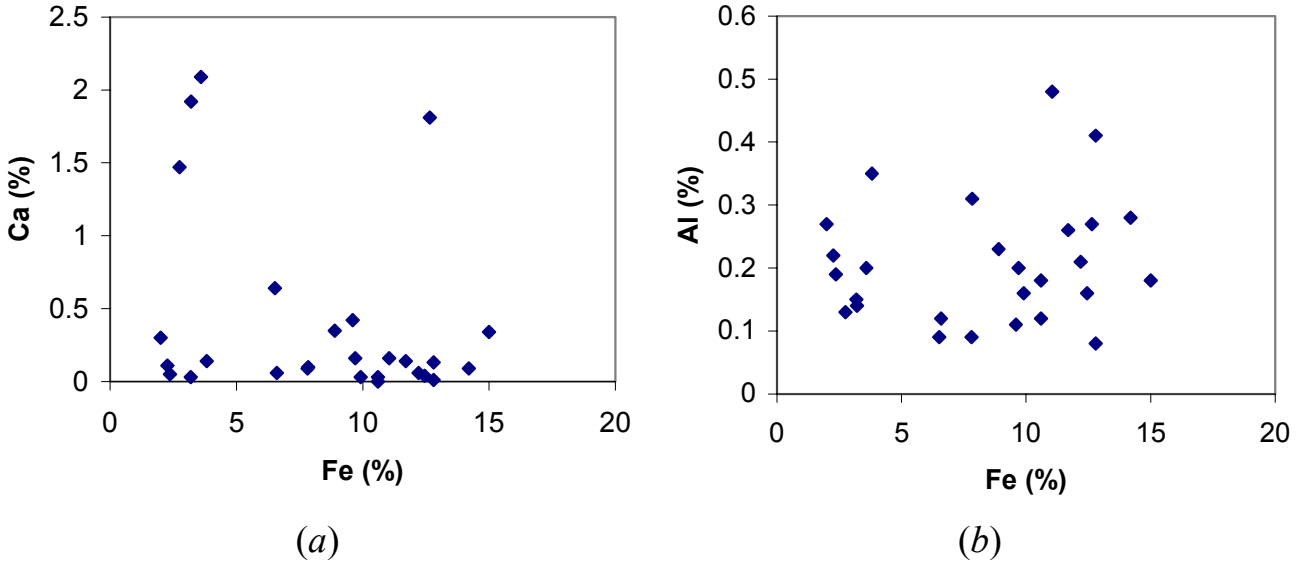

Figure 9. Bivariate plots of different elements in the Wajid Sandstone: (a) *Fe and Ca and* (b) *Fe and Al. The trend of negative correlation between Ca and Fe is consistent with the petrographic observation of replacement of calcite cement by hematite and goethite.*

In addition to the ironstone samples, some samples (mainly felsic to intermediate plutonic rocks) from the underlying basement complex were analyzed (Table 3). The concentrations of Fe, Al, and Ca range from 0.49 to 5.42%, 0.23 to 2.75%, and 0.07 to 1.95%, respectively. Other major elements including Mg, K, Ti, and Na are generally very low, ranging between <0.01 and 2.62%. The concentration of Fe_2O_3 ranges from 0.85 to 14.05% while the values of CaO, and MgO, range from 0.2 to 21.5% and 0.11 to 13.73%, respectively. The trace elements Cr, Ni, Co, V, and Sr range from 26 to 387 ppm, 2 to 287 ppm, 1 to 105 ppm, and 2 to 95 ppm, respectively.

The relative concentrations of selected elements in the ironstone were compared with those of the local basement rocks in study area, and hydrothermal fluids [17; Figure 10] to determine the possible source of iron in the Wajid Sandstone. As shown in Figure 10, the distribution of Fe in the ironstone appears to be similar to that of the basement rocks especially the gabbroic rocks. The enrichment of iron in both the ironstone and gabbroic rocks may indicate that the iron in the ironstone was sourced by the alteration of ferromagnesian minerals in the gabbroic and other basic and ultrabasic rocks. On the other hand, the concentrations of Mg in the gabbroic rocks are significantly higher indicating some other likely sources such as hydrothermal fluids.

Table 3. Elemental Chemistry of the Basement Complex Samples.

Sample	Al (%)	Ba (ppm)	Ca (%)	Co (ppm)	Cr (ppm)	Cu (ppm)	Fe (%)	Fe (ppm)	K (%)	La (ppm)	Mg (%)	Mn (ppm)	Mo (ppm)	Na (%)	Na (ppm)	Ni (ppm)	P (ppm)	Sc (ppm)
B1	2.61	40	1	21	129	30	5.04	50400	0.1	<10	1.44	740	3	<.01	100	25	980	4
B2	1.69	20	1.33	24	387	86	2.97	29700	0.02	30	2.62	360	2	0.05	500	281	1750	17
B3	1.76	170	0.61	7	44	4	2.74	27400	0.84	40	0.87	300	2	0.01	100	21	1620	4
B4	0.99	70	11.95	5	52	11	1.7	17000	0.23	40	0.73	225	3	0.46	4600	5	590	3
B5	0.23	<10	0.03	2	154	6	4.92	49200	0.03	<10	0.01	30	1	<.01	100	11	90	3
B6	0.32	10	0.06	1	77	6	0.49	4900	0.04	<10	0.08	75	<1	0.04	400	3	70	<1
B7	0.7	30	0.13	<1	26	<1	0.52	5200	0.22	50	0.07	25	1	0.01	100	2	130	1
B8	0.37	10	1.4	1	75	7	1.23	12300	0.14	60	0.13	215	3	0.25	2500	9	210	1
B9	2.9	30	0.88	43	93	32	5.27	52700	0.09	<10	1.54	915	4	<.01	100	47	1310	5
B10	0.32	<10	0.07	1	103	4	0.62	6200	0.03	10	0.03	30	1	<.01	100	4	100	<1
B11	2.75	20	0.86	29	123	46	5.42	54200	0.29	<10	1.51	810	3	<.01	100	24	950	5

Sample	Sr (ppm)	Ti (%)	V (ppm)	Zn (ppm)	Al_2O_3 (%)	CaO (%)	Cr_2O_3 (%)	Fe_2O_3 (%)	K_2O (%)	MgO (%)	MnO (%)	Na_2O (%)	P_2O_5 (%)	SiO_2 (%)	TiO_2 (%)	LOI (%)	TOTAL	CIA
B1	20	0.49	92	74	13.99	7.72	0.02	13.15	0.51	6.26	0.21	3.73	0.18	49.54	1.98	2.59	99.88	53.9
B2	61	0.16	36	32	8.29	9.2	0.11	9.03	0.95	13.8	0.14	1.52	0.36	50	1.19	6.29	100.85	41.5
B3	28	0.18	48	98	15.6	2.7	0.01	3.89	3.73	1.5	0.05	4.03	0.35	64.58	1.32	2.05	99.8	59.9
B4	95	0.15	41	24	10.5	21.5	0.01	3.59	1.67	1.86	0.06	3.26	0.12	39.21	0.47	18.1	100.3	28.4
B5	2	<.01	20	8	2.23	0.05	0.02	7.01	0.25	0.08	0.01	0.04	0.01	89	0.05	1.52	100.25	86.8
B6	4	<.01	4	8	15.71	0.2	0.01	0.85	1.88	0.19	0.01	6.88	0.01	73.18	0.1	1.01	100	63.7
B7	14	<.01	1	10	12.92	0.19	0.01	1.12	6.19	0.31	0.06	0.09	0.01	76	0.15	3.36	100.4	66.6
B8	16	0.04	4	30	13.13	2.45	0.01	1.79	5.16	0.22	0.05	3.87	0.04	71.6	0.16	2.46	100.95	53.4
B9	24	0.28	69	92	15.42	7.91	0.01	13.02	0.77	5.32	0.22	2.44	0.27	48.93	1.96	3.53	99.8	58.1
B10	4	<.01	8	2	7.49	0.09	0.01	1.12	0.32	0.11	0.01	0.05	0.01	86.6	0.11	3.02	98.94	94.2
B11	21	0.5	105	76	13.75	7.39	0.02	14.05	0.55	6.32	0.24	3.51	0.19	47.05	2.03	3.24	98.34	54.6

Sample Identities: B1: Diorite; B2: Gabbro; B3, B9, and B11: Mica Schists; B4: Biotite Gneiss; B5, B6, and B10: Pegmatite; B7: Talc (?); B8: Granite.

The distribution of As and Ba in the ironstone was also compared (Figure 11) with that of the basement rocks, and also the hydrothermal fluids to ascertain possible contribution of hydrothermal solutions in enrichment of iron in the Wajid Sandstone. These elements show relatively high concentrations in the ironstone, the gneiss and schist samples analyzed (Figure 11). The distribution of these elements in the ironstone appears comparable to that of the modern hydrothermal solutions than that in the basement rocks suggesting part of the iron in the Wajid Sandstone have derived from hydrothermal fluids.

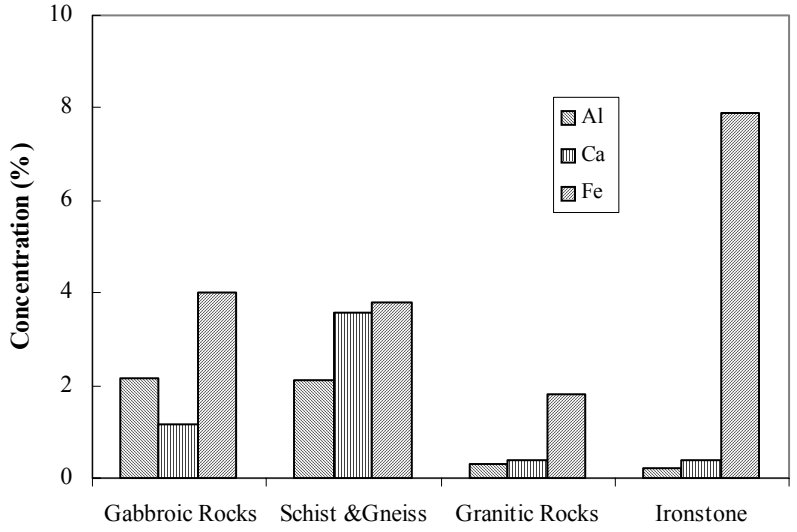

(*a*)

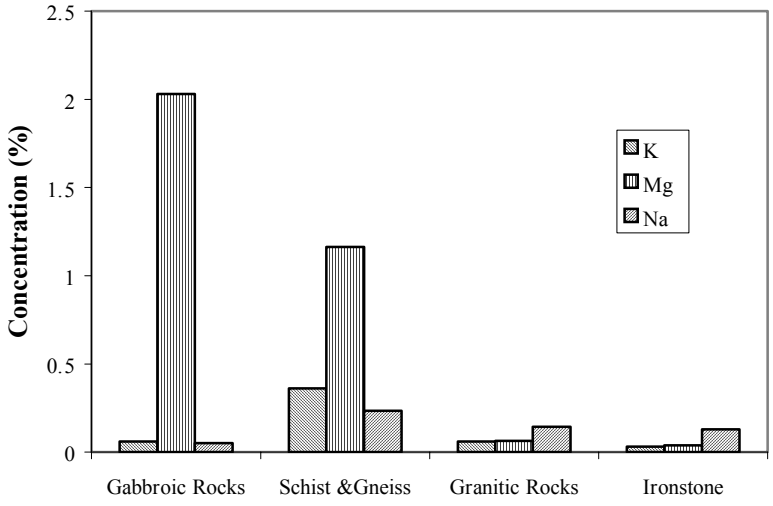

(*b*)

Figure 10. Distribution of some major elements in the basement rock types and ironstone samples in the study area: (a) *distribution of Al, Ca, and Fe in different rock types in the basement complex and ironstone samples; and* (b) *distribution of K, Mg, and Na in the different rock types in the basement complex and ironstone samples. The concentrations of Fe in the ironstone and gabbroic rocks in the study area are comparable suggesting ferromagnesian minerals in the mafic rocks, as a source of iron in the iron-rich samples in the Wajid Sandstone.*

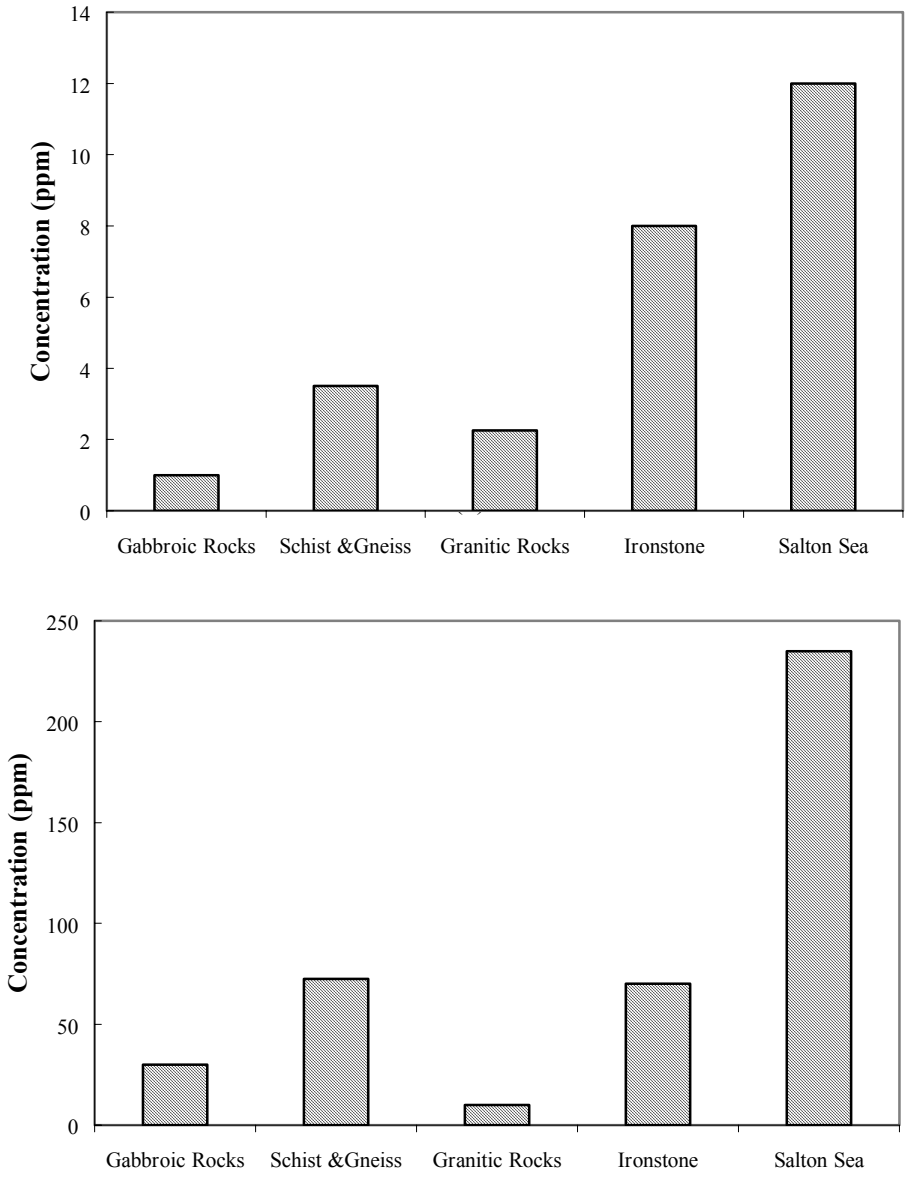

Figure 11. Distribution of As and Ba in the ironstone, basement complex samples, and modern hydrothermal solutions from the Salton Sea (hydrothermal solutions data were obtained from Guilbert and Park [17]): (a) *concentrations of As; and* (b) *concentrations of Ba. Note that the concentrations of these elements in the ironstone are comparable to those of the hydrothermal solutions.*

7. DISCUSSION

Many different models have been proposed in recent years to explain the enrichment of iron in sedimentary sequences including Precambrian banded iron formations [18]. Among the more widely cited models are: (*i*) subaerial weathering of continental rocks [19–21]; (*ii*) upwelling water [22, 23]; (*iii*) submarine volcanic or hydrothermal exhalation [24–28]; and (*iv*) diagenetic water [29–32]. The validity of a particular model tied to many factors including the geologic and tectonic history of the area [33]. In-situ conversion of goethite/limonite cements [34–38] or post-depositional intrastratal dissolution of iron-rich mafic minerals including hornblende, biotite, pyroxene, olivine, and epidote [39–41] are also possible mechanism of iron enrichment. The corroded nature of feldspars and hornblende grains, as observed in thin section petrography, reinforce such interpretations.

The absence of labile minerals such as pyroxene and olivine indicates the role of intrastratal alteration and weathering processes in modifying the mineralogical composition of the Wajid Sandstone. The replacement of early calcite cement by iron minerals, as observed in thin-section petrographic study suggests a diagenetic origin of the iron in the ironstone in the Wajid Sandstone. The preservation of delicate textural and morphological features in iron minerals like hematite and goethite in the ironstone also favors an in-situ, diagenetic origin for the iron.

The basement complex in the study area comprises a variety of mafic rocks including gabbro, basalt, and amphibolite. In addition, the shield area to the south also contains abundant outcrops of mafic rocks [1]. Igarashi [42] reported the occurrence of iron ore from the Jabal Al-Soudah, one of the localities investigated in this study. Thus, the mafic and ultramafic rocks of the Arabian Shield are a likely source of iron in the Wajid Sandstone. The observed high concentrations of Fe, in the ironstone and local gabbroic rocks analyzed, favors likely derivation of Fe from ferromagnesian minerals in the gabbroic and other mafic rocks in the study area. Textural and petrographic study shows that part of the Wajid Sandstone is poorly-sorted and is composed of abundant angular, coarse sand to pebble-size particles, indicating a nearby source [5]. Although the source area in the vicinity contains abundant mafic and intermediate igneous rocks, the sandstone is almost free of any ferromagnesian minerals. The maturity of the framework minerals and high chemical index of alteration (CIA) recorded in the Wajid Sandstone [6] suggest intense chemical weathering of the Wajid Sandstone. This intensive weathering is likely to have degraded the labile, ferromagnesian, minerals in the Sandstone and released the iron that now forms the iron-rich horizons.

Numerous plutons and hydrothermal veins characterize the basement complex at the study area. Several authors including Gross and Zajac [43], Peter and Goodfellow [44], and Peter [45] discussed the role of hydrothermal activity in ironstone formation. Peter [45] suggested that buoyant plumes, formed by hydrothermal fluids, can create banded sulfide ores and associated ferrugineous cherts, jaspers, jasperoids, cherty tuffs, tuffites, tuffaceous exhalites, chloritic iron formations, or sulfide iron formations may also form *via* hydrothermal activity.

According to Johnson *et al*. [13], volcanic/plutonic activity in the Asir terrain continued until 606 ± 2 Ma. The presence of pegmatite veins in the basal part of the Wajid Sandstone and the occurrence of kaolinite horizons in the transition zone between the Wajid and basement complex, as reported in the present study indicate that volcanic activity in the area continued even after the deposition of the basal units of the Wajid Sandstone. The level in the concentrations of As and Ba in the ironstone and those of modern hydrothermal solutions may also indicate that of the Fe in the Wajid Sandstone was partly derived from hydrothermal activity. Hydrothermal activity in the area is also indicated by the presence of jasper clasts in the ironstone intervals within the Sandstone. Thus, part of the Fe in the ironstone might have derived from the Proterozoic basement rocks *via* hydrothermal circulation or volcanic exhalation [46; personal communication]. In addition, hot hydrothermal fluids not only aided dissolution of the labile ferromagnesian minerals in the Wajid Sandstone, but also helped in mobilizing the iron-bearing fluids and formation of the ironstone. The fact that the distribution of ironstone is largely confined to the Red Unit implies that hydrothermal activities associated with the basement complex were either not active or less active during/after the deposition of the overlying Grey Unit. Alternatively, a change to an iron-poor provenance may also explain the lesser volume of iron in the Grey Unit. Considering the stratigraphic position of the Wajid Sandstone and the regional orogenic events in the region, the hydrothermal activity responsible for the mobilization and emplacement of iron may be related to the InfraCambrian Najd Rifting event in the area [47].

CONCLUSIONS

The iron-rich horizons in the Wajid Sandstone consist of quartz sandstone cemented and coated with iron. The concentration of iron (Fe) in the Sandstone varies from ~9% to over 15%. Based on the petrographic evidence, including near to complete absence of labile and ferromagnesian minerals, the presence of degraded ferromagnesian minerals like hornblende and feldspar, and the abundance of monomineralic (kaolinite) clay with well-preserved textural and morphological features all suggest [48] that labile, ferromagnesian minerals in the sandstone acted as the main source for iron in the Sandstone. Replacement of calcite cement by ferruginous cement and the negative correlation between Fe and Ca ions both indicate a diagenetic origin of the iron. Additional sources of iron include weathering of

the mafic and intermediate rocks of the basement complex. Geochemical evidence mainly the association of trace elements such as Cr, Co, Ni, Cu, and V, also favor a mafic source.

The basement complex in the area, as well as the basal section of the Red Unit of the Wajid Sandstone are characterized by the presence of pegmatite veins suggesting the continuation of hydrothermal activity into the early part of the Paleozoic. Abundant iron-rich horizons in the Red Unit, coupled with presence of jasper clasts in the ironstone, and patches of kaolin atop of the basement complex all suggest the role of hydrothermal fluids in mobilizing and emplacing the iron. Based on the regional tectonic history of the region, the hydrothermal activity responsible for the formation of the ironstone appears to be associated with the InfraCambrian to Cambrian Najd Rifting event.

ACKNOWLEDGEMENTS

The authors would like to thank Dr. Peter Johnson of the Saudi Geological Survey and Professor John K. Warren of the University of Brunei for sharing their expertise in improving the technical quality of the manuscript. Constructive review and suggestions by two anonymous reviewers also helped in clarifying the technical details of the paper. A number of graduate students of the Earth Sciences Department at KFUPM, including Mr. Waleed Hasan, Mr. Jowaher Raza, and Mr. Aamir Siddique, have been of great assistance both in the field and during the preparation phase of the paper. Finally, the authors would like to acknowledge KACST and KFUPM for supporting the research.

REFERENCES

[1] G.F. Brown, D.L. Schmidt, and A.C. Huffman (Jr.), "Geology of the Arabian Peninsula — Shield Area of the Western Saudi Arabia", *US Geological Survey Professional Paper 560 A*, 1989, A188p.

[2] M.A. Moshrif and A. El-Hiti, "Lithofacies and Petrography of Wajid Sandstone (Cambrian–Ordovician) Saudi Arabia", *Journal of African Earth Sciences,* **9**(**2**/**4**) (1989), pp. 42–72.

[3] T.E Stump and J.G. van der Eem, "Overview of the Stratigraphy, Depositional Environments and Periods of Deformation of the Wajid Outcrop Belt, Southwestern Saudi Arabia", *Proceedings Geo Arabia Conference,* 1994, pp. 867–876.

[4] W.R. Greenwood, "Explanatory Notes to the Geologic Map of the Abha Quadrangle", Sheet 18F: Saudi Arabian Directorate General of Mineral Resources, Kingdom of Saudi Arabia, accompanying 1:250,000 scale geologic map GM-75C, 1985, text 27p.

[5] L.O. Babalola, "Depositional Environments and Provenance of the Wajid Sandstone, Abha–Khamis Area, Southwestern Saudi Arabia", *MS Thesis, King Fahd University of Petroleum and Minerals, Saudi Arabia,* 1999, 239p.

[6] M. Hussain, L.O. Babalola, and M.M. Hariri, "Provenance of the Wajid Sandstone, Southeastern Margin of the Arabian Shield: Geochemical and Petrographic Approach", *American Association of Petroleum Geologists Conference, New Orleans, USA,* April 16, 2000. Extended Abstracts with Programs: 7p.

[7] H.L. James, "Sedimentary Facies of Iron-Formation", *Economic Geology*, **49** (1954), pp. 235–293.

[8] P. Johnson, "Perozoic Geology of the Saudi Arabia: Current Concepts and Issues" *Contribution to a Workshop on the Geology of the Arabian Peninsula, 6th Meeting of the Saudi Society for Earth Sciences, King AbdulAziz City for Science and Technology, Riyadh*, February 1, 2000.

[9] D.B. Stoeser, M.J. Whitehouse, and J.S. Stacey, "The Khida Terrane — Geology of Paleoproterozoic Rocks in the Muhayil Area, Eastern Arabian Shield, Saudi Arabia", *Gondowana Research*, **4** (2001), pp.192–194.

[10] J.G. McGillivrary and M.I. Husseini, The Paleozoic Petroleum Geology of Central Arabia, *American Association of Petroleum Geologists Bulletin,* **76** (1992), pp.1475–1490.

[11] P.J. Jones and T.E. Stump, "Depositional and Tectonic Setting of the Lower Silurian Hydrocarbon Source Facies, Central Saudi Arabia", *American Association of Petroleum Geologists Bulletin,* **82**(**2**) (1999), pp. 314–332.

[12] M.E. Dabbagh and J.W. Rogers, "Depositional Environments and Tectonic Significance of the Wajid Sandstone of Saudi Arabia", *Journal of African Earth Sciences,* **1** (1983), pp. 47–57.

[13] P.R. Johnson, H.K. Fayek, and J.L. Wooden, "Implication of SHRIMP and Microstructural Data on the Age and Kinematics of Shearing in the Asir Terrane, Southern Arabian Shield, Saudi Arabia", *Gondowana Research*, **4**(**2**) (2001), pp. 172–173.

[14] M. Hussain, L.O. Babalola, and M.M. Hariri, "Ironstone in the Wajid Sandstone: An Example of Hydrothermally-Induced Iron Accumulation in a Sedimentary Sequence", *International Symposium and Field Workshop: Tectonics and Mineralization in the Arabian Shield and its Extensions, UNESCO–IGCP Project 368: Proterozoic Events in East Gondowana, Gondowana Research,* March 14–16, 2001, Abstracts (Addendum).

[15] K.S. Kellog, J. Fourniguet, J. Janjou, and L. Minoux, "Geologic Map of the Wadi Tathlith Quadrangle, (Sheet-20G, Saudi Arabia)", *Saudi Arabian Deputy Ministry for Mineral Resources, Map G.M-103C.,* 1986.

[16] M.A. Morsy, "An Example of Application of Factor Analysis on Geochemical Stream Sediment Survey in Umm Khariga Area, Eastern Desert, Egypt", *Mathematical Geology*, **25** (1993), pp. 833–850.

[17] J.M. Guilbert and C.F. Park (Jr.), *The Geology of Ore Deposits*. New York: Freeman and Company, 1986, 985p.

[18] Y.P. Mel'nik, *Precambrian Banded Iron-Formations*. New York: Elsevier, 1982, 310p.

[19] H. Lepp and S.S. Goldich, "Origin of Precambrian Iron Formation", *Economic Geology,* **58** (1964), pp. 1025–1061.

[20] P.E. Cloud, **"**Paleoecological Significance of Banded Iron Formations", *Economic Geology,* **68** (1973), pp.1135–1143.

[21] H. Lepp, "Chemistry of Iron: Precambrian Iron Formation", in *Precambrian Iron Formation.* ed. P.W.U Appel and G.I. LaBerge. Athens, Greece: Theophastus, S.A., 1987, pp. 3–30.

[22] J.I. Drever, "Geochemical Model for the Origin of Precambrian Banded Iron Formations", *Geological Society of America Bulletin,* **85** (1974), pp.1099–1106.

[23] A. Button, T.D. Brock, P.J. Cook, H.P. Eugster, A.M. Goodwin, H.L. James, I. Margulis, K.H. Nealson, J.O. Nriagu, A.F. Trendall, and M.R. Walter, "Sedimentary Iron Deposits, Evaporites and Phosphorites", in *Mineral Deposits and Evolution of Biosphere.* ed. H.D. Holland and M. Schidlowski. New York: Springer-Verlag, 1982, pp. 259–273.

[24] R. Bostrom, "Submarine Volcanism as a Source of Iron", *Earth Planetary Science Letter,* **9** (1970), pp. 348–354.

[25] A. Hajash, "Hydrothermal Processes along Mid-Ocean Ridges: An Experimental Investigation", *Contributions to Mineralogy and Petrology,* **53** (1975), pp. 205–226.

[26] D.Z. Piper, "An Iron-Rich Deposit from the Northeastern Pacific", *Earth and Planetary Science Letters*, **26** (1975), pp. 114–120.

[27] G.A. Gross, "A Classification of Iron Formation Based on Depositional Environments", *Canadian Mineralogist,* **18** (1980), pp. 215–222.

[28] B.M. Simonson, "Sedimentological Constraints on Origin of Precambrian Iron Formations", *Geological Society of America Bulletin,* **96** (1985), pp. 224–252.

[29] M.M. Kimberley, "Origin of Oolitic Iron Formation", The Society of Economic Geologists, Paleontologists and Mineralogists, 79 (1979), pp. 111–131.

[30] D.A. Spears, **"**Aspects of Iron Incorporation into Sediments with Special Reference to the Yorkshire Ironstones", in *Phanerozoic Ironstones.* ed. T.P. Young and W.E.G. Taylor. Geological Society Special Publication, **46** (1989), pp.19–30.

[31] T.P. Young, "Sedimentary Ironstones", in *Mineralization in Britain*. ed. R.A.D. Patrick and D.A. Poyla. London: Chapman and Hall, 1993, pp. 446–489.

[32] E. Cotter and J.E. Link, "Deposition and Diagenesis of Clinton Ironstones (Silurian) in the Appalachian Foreland Basin of Pennsylvania", *Geological Society of America Bulletin,* **105** (1994), pp. 911–922.

[33] A.F. Trendall and R.C. Morris (eds.), *Iron-Formation: Facts and Problems*. New York: Elsevier, 1983, 558p.

[34] F.B. van Houten, "Origin of Red Beds — Some Unresolved Problems", in *Problems in Paleoclimatology, Proceedings of NATO Paleoclimates Conference*. ed. A.E.M. Nairn. New York: Interscience, **163** (1964), pp. 647–661.

[35] F.B. van Houten, "Iron Oxides in Red Beds", *Geological Society America Bulletin,* **79** (1968), pp.399–416.

[36] F.B. van Houten, "Iron and Clay in Tropical Savanna Alluvium, Northern Colombia: a Contribution to the Origin of Red Beds", *Geological Society of America Bulletin,* **83** (1972), pp. 2761–2772.

[37] F.B. van Houten, "Origin of Red Beds: A Review — 1961–1972", *Annual Review of Earth and Planetary Science,* **1** (1973), pp. 39–61.

[38] R.A. Berner, "Goethite Stability and the Origin of Red Beds", *Geochimica et Cosmochimica Acta,* **33** (1969), pp. 267–273.

[39] T.R. Walker, **"**Formation of Red Beds in Modern and Ancient Deserts", *Geological Society of America Bulletin,* **78** (1973), pp. 353–368.

[40] T.R. Walker, **"**Intrastratal Alterations in the Fountain Formation (Pennsylvanian age), Denver Area, Colorado", *Geological Society of America, Abs. With programs (Southwestern Section),* **5** (1973), pp. 521–522.

[41] T.R. Walker and R.M. Honea, "Iron Content of Modern Deposits in the Sanoran Desert: a Contribution to the Origin of Red Beds", *Geological Society of America Bulletin,* **80** (1969), pp. 535–544.

[42] T. Igarashi, "Mineral Reconnaissance of the Ablah-AlAlayyah Area and the Abha District", in *Mineral Resources Research 1967-1968.* Riyadh: Ministry of Petroleum and Mineral Resources, Directorate General of Mineral Resources, 1969, pp. 8–10.

[43] G.A. Gross and I.S. Zajac, "Iron-Formation in Fold Belts Marginal to the Ungava Craton", in *Iron-Formation: Facts and Problems*. ed. A.F. Trendall and R.C. Morris. Amsterdam: Elsevier, 1983, pp. 253–294.

[44] J.M. Peter and W.D. Goodfellow, "Mineralogy, Bulk and Rare Element Earth Geochemistry of Massive Sulphide-Associated Hydrothermal Sediments of the Brunswick Horizon, Bathurst Mining Camp, New Brunswick", *Canadian Journal of Earth Sciences*, **33** (1996), pp. 252–283.

[45] J.M. Peter, "Hydrothermal Sediments", *EXTECH-II Project Report, Mineral Resources Division, Geological Survey of Canada*, 2001, Section 1–6.

[46] P. Johnson, Saudi Geological Survey, Jeddah, Personal Communication, 2000.

[47] M.D. Wilson and E.D. Pittman, "Authigenic Clays in Sandstone: Recognition and Influence of Reservoir Properties and Paleoenvironmental Analysis", *Journal of Sedimentary Petrology*, **47** (1977), pp. 3–31.

[48] M.A. Abu-Ali, J.L. Rudkiewicz, J.G. McGillivrary, and F. Beha, "Paleozoic Petroleum Systems of Central Arabian", *GeoArabia*, **4** (1999), pp. 321–326.

Paper Received 29 January 2001; Revised 17 March 2002; Accepted 27 May 2002.